Relativistic Love-Franey model: Covariant representation of the NN interaction for N-nucleus scattering

C. J. Horowitz*
Department of Physics, University of Colorado, Boulder, Colorado 80309
and Center for Theoretical Physics and Department of Physics, Massachusetts Institute of Technology, Cambridge, Massachusetts 02139
(Received 17 October 1984)

A Lorentz invariant form of the NN amplitude is fit with a simple model which includes direct and exchange first Born terms from a number of "mesons." The (complex) couplings and nucleon-meson form factors are adjusted to fit the NN amplitudes directly without iteration. The resulting parameters agree well with one-boson-exchange potentials and have a systematic and small energy dependence. Detailed analytic representations of the relativistic NN amplitudes are provided at lab energies of 135, 200, and 400 MeV. The model separation of the NN amplitudes into direct and exchange contributions does not involve sensitive cancellations and is contrasted with the very different nonrelativistic results. The model amplitudes are used to construct optical potentials in a relativistic impulse approximation using both pseudovector and pseudoscalar π-N coupling. The pseudoscalar result reproduces earlier relativistic impulse approximation calculations which diverge at low energies, while the pseudovector results are nearly constant with energy and in good agreement with phenomenological potentials.

I. INTRODUCTION

Recently, a number of relativistic approaches to nucleon-nucleus scattering have shown the importance of correctly treating the strong relativistic interactions. Relativistic impulse approximation (RIA) (Ref. 1) as well as mean field theory (MFT) (Ref. 2) calculations, give a N-nucleus optical potential which has Lorentz scalar and vector components of order one-half the nucleon mass (and opposite signs). Furthermore, these strengths are important in correctly describing spin observables.

However, RIA calculations to date have not explicitly treated exchange contributions, have suffered from ambiguities in the relativistic form of the NN amplitudes,[3] and have, for the most part, been limited to elastic scattering. In this paper, a simple model with explicit exchange terms is fit to the relativistic NN amplitudes. This allows one to examine different off-shell extrapolations in the exchange terms. Furthermore, the simplicity of the model may be very useful in relativistic inelastic scattering calculations. Finally, the model allows one to examine a number of relativistic ambiguities in the NN amplitudes.

The commonly used McNeil-Ray-Wallace (MRW) (Ref. 4) form of the relativistic amplitudes is completely local and thus cannot fully treat the nonlocalities that must be there from exchange. At lab energies of 500 MeV and above (where the RIA works well), this appears to be a good approximation. But, as the energy is lowered, this incorrect treatment of exchange must fail. Indeed, the scalar and vector optical potentials from the RIA diverge at energies below 100 MeV, becoming much greater than phenomenological optical potentials (which are nearly constant with energy[5]).

An important step in RIA calculations (see the following) is to equate four component spinor matrix elements of some two-nucleon operator to the NN amplitudes. Then, the projectile spinors are stripped away and the bare operator used to construct an optical potential. The problem is that there are an infinite class of operators which have the same free spinor matrix elements but which give different optical potentials. Thus, the N-nucleus observables calculated in the RIA depend explicitly on the assumed (arbitrary) form of the NN operator used to represent the amplitudes. Therefore, it is important to have a simple model of this operator where one can examine carefully the assumptions made about its form.

Our model for the NN interaction considers the exchange of a number of "mesons" in first Born approximation including both the direct and exchange NN scattering diagrams. The meson couplings (complex) and meson-nucleon form factors are adjusted until the relativistic representation[4] of the Arndt amplitudes[6] is reproduced directly without iteration of the meson exchanges.

The motivation for this procedure is severalfold. First, the fit provides a simple analytic form which may be useful in calculations and a detailed examination of different off-shell extrapolations. Second, the fit gives a model separation of direct and exchange contributions to allow systematic improvements in the treatment of exchange in nucleon-nucleon scattering.

The assumptions the model makes about the relativistic form of the NN amplitudes are very simply related to the type of meson-nucleon vertices used. Therefore we easily study the sensitivity of the resulting RIA optical potential to different vertices. (For example, the differences between pseudoscalar and pseudovector π-N coupling.) In addition, the parameters from the fit are very close to couplings of one boson exchange potentials (OBEP's).

Thus, our model separation of direct and exchange contributions is expected to be close to the results of a full OBEP.

We are interested in the Lorentz structure of the NN amplitudes (how the net amplitude is divided into Lorentz scalar, vector, etc., pieces). First Born approximation has proven to be a good guide for the Lorentz structure of the optical potential or self-energy. The scalar self-energy is almost unchanged when relativistic mean field calculations are replaced by full Brueckner calculations.[7] Thus, Born approximations may be a useful first representation of the structure of the NN amplitudes.

There are a number of significant advantages of a relativistic approach over the conventional nonrelativistic work of Love and Franey,[8] where the NN interaction is represented by an arbitrary sum of Yukawa functions. First, there is a simple relationship between the individual Lorentz invariant amplitudes and the mesons exchanged which is lacking in the nonrelativistic treatment. Second, the parameters of the fit may be more meaningful since they are close to OBEP values, and have a systematic and small energy dependence. There is no sensitive cancellation between direct and exchange contributions (see Sec. IV). In contrast, the Love-Franey fits have individual direct and exchange terms which are an order of magnitude larger than the net. Finally, our fit is Lorentz covariant and allows one to correctly treat strong relativistic optical potentials.

In Sec. II, the formalism of our fit is presented. Then, in Sec. III, detailed results are presented for lab energies of 135, 200, and 400 MeV. This section also shows the quality of the NN observables produced. The model separation of direct and exchange contributions is discussed in Sec. IV and contrasted with the very different nonrelativistic results, while Sec. V uses the amplitudes to construct RIA optical potentials for both pseudoscalar and pseudovector π-N vertices. We find that our explicit treatment of exchange together with pseudovector pion coupling leads to optical potentials in good agreement with phenomenology. Our conclusions are in Sec. VI.

II. FORMALISM FOR THE NN AMPLITUDE

Since there is only a limited amount of information in the NN phase shifts, one needs an explicit model of the NN amplitude to learn about its Lorentz structure and off-shell behavior. In principle, a OBEP model completely determines the full Dirac structure of an off-shell t matrix and, indeed, such calculations are underway.[9,10] However, the complexity of this program has limited physical insight into the resulting amplitudes. Furthermore, most of the justification for one-boson exchange (OBE) models has come from their reproducing of on-shell NN data. Predictions for the off-shell, or Lorentz structure of the NN amplitudes, need not be correct since they have never been tested. Therefore, the extra complexity of the full calculations may not be justified. Instead, we work with a simple model that reproduces the same NN data and has coupling constants close to those of OBE models. Because our couplings are similar, this simple model may give results close to those of a full OBEP.

Our starting point is the conventions of McNeil, Ray, and Wallace[4] for the NN amplitudes

$$(2ik_c)^{-1}f_c = A + B\sigma_1\cdot\sigma_2 + iqC(\sigma_{1n}+\sigma_{2n}) + D\sigma_1\cdot q\sigma_2\cdot q + E\sigma_{1z}\sigma_{2z} \ . \tag{1}$$

Here, f_c is the nonrelativistic amplitude, $A, \ldots, E$ are the Wolfenstein amplitudes, and k_c is the momentum in the c.m. frame. This is then equated to the Dirac spinor (U) matrix elements of the relativistic amplitude $\hat{F}$,

$$(2ik_c)^{-1}f_c = \bar{U}_1\bar{U}_2\hat{F}U_1U_2 \ , \tag{2}$$

represented with the set of Lorentz invariants (i: s=scalar, v=vector, p=pseudoscalar, a=axial vector, and t=tensor).

$$\hat{F} = \sum_{i=s}^{t} \lambda^i_{(1)}\lambda^i_{(2)}F^i \ ,$$

i	λ^i
s	1
v	γ^μ
p	γ^5
a	$\gamma^5\gamma^\mu$
t	$\sigma^{\mu\nu}$.

(3)

Our gamma matrix conventions are those of Ref. 11. The optical potential in an impulse approximation is given by [see Sec. V and Ref. 1]

$$U_{\rm opt} = -4\pi i\left[\frac{p}{M}\right](F^s\rho_s + \gamma^0F^v\rho_b) \ , \tag{4}$$

where p is the momentum of the projectile and ρ_s is the scalar and ρ_b the baryon density of the target.

We fit the invariants F^i with direct plus exchange contributions

$$F^i = i\frac{E_{\rm c.m.}}{2p_{\rm c.m.}}[F^i_D(q)+F^i_{\rm ex}(Q)] \ . \tag{5}$$

Note the kinematic factor where $2p_{\rm c.m.}=(2T_{\rm lab}M)^{1/2}$, with $T_{\rm lab}$ the projectile's kinetic energy, $E_{\rm c.m.}=[p^2_{\rm c.m.}+M^2]^{1/2}$, and the direct momentum transfer q for scattering angle $\theta_{\rm c.m.}$ is

$$q = 2p_{\rm c.m.}\sin(\theta_{\rm c.m.}/2) \ , \tag{6}$$

while the exchange momentum transfer Q is

$$Q = 2p_{\rm c.m.}\sin\left[\frac{\pi-\theta_{\rm c.m.}}{2}\right] \ . \tag{7}$$

For the direct contribution, we use

$$F^i_D(q) = \sum_{j=1}^{N}\delta_{i,{\rm type}_j}(\tau_1\cdot\tau_2)^{I_j}f^j(q) \ , \tag{8}$$

where

$${\rm type}_j = \text{kind of meson—N coupling for the } j\text{th meson} \ , \tag{9a}$$

$$(s,\ v,\ t,\ a,\ \text{or}\ p) \ ,$$

$$N = \text{number of mesons used in fit} \ , \tag{9b}$$

I_j = isospin of jth meson (0 or 1) , (9c)

$$f^j(q)=f^j_R(q)-if^j_I(q) , \tag{9d}$$

$$f^j_R(q)=\frac{g_j^2}{q^2+m_j^2}(1+q^2/\Lambda_j^2)^{-2} , \tag{9e}$$

$$f^j_I(q)=\frac{\bar{g}_j^2}{q^2+\bar{m}_j^2}(1+q^2/\bar{\Lambda}_j^2)^{-2} , \tag{9f}$$

with m_j being the meson mass and parameters g_j^2 and Λ_j fit to data. For the imaginary parts, one has the new parameters $\bar{m}_j$, $\bar{g}_j^2$, and $\bar{\Lambda}_j$.

For the exchange terms, we rewrite exchange Lorentz invariants in terms of the five direct invariants of Eq. (3). This is known as a Fierz transformation.[12] To start, consider the exchange contribution of a scalar meson. The elementary Feynman rules [see, for example, (2)] put a factor at each vertex proportional to the unit matrix. This gives a $4\times4\oplus4\times4$ matrix contribution to the NN amplitude which depends on

$$[1]_{12'}[1]_{21'} . \tag{10}$$

Here the 1 (1′) index refers to the initial (final) spinor of particle one. This is expanded

$$[1]_{12'}[1]_{21'}=\sum_j C_{sj}\lambda^j_{11'}\lambda^j_{22'} , \tag{11}$$

or, in general,

$$\lambda^k_{12'}\lambda^k_{21'}=\sum_j C_{kj}\lambda^j_{11'}\lambda^j_{22'} , \tag{12}$$

and the Fierz matrix C is

$$C_{kj}=\mathrm{tr}(\lambda^k\lambda^j\lambda^k\lambda^j)/[\mathrm{tr}[\lambda^j\lambda^j]]^2 ,$$

$$C=\frac{1}{8}\begin{bmatrix} 2 & 2 & 1 & -2 & 2 \\ 8 & -4 & 0 & -4 & -8 \\ 24 & 0 & -4 & 0 & 24 \\ -8 & -4 & 0 & -4 & 8 \\ 2 & -2 & 1 & 2 & 2 \end{bmatrix}\begin{bmatrix} s \\ v \\ t \\ a \\ p \end{bmatrix} . \tag{13}$$

Note that $C\cdot C=1$ since the exchange of the exchange leaves the nucleons in the original order. Since both C_{ss} and $C_{sv}=\frac{1}{4}$ the exchange contribution from a scalar meson will contribute to both scalar F_s and vector F_v invariants with equal weights. In contrast, the exchange terms from a vector meson lead to a large scalar contribution ($C_{vs}=1$) and a vector contribution of opposite sign ($C_{vv}=-\frac{1}{2}$).

Using this matrix, one has

$$F^i_{\mathrm{ex}}(Q)=(-1)^{I_{\mathrm{NN}}}\sum_j C_{\mathrm{type}_j,i}(\tau_1\cdot\tau_2)^{I_j}f^j(Q) , \tag{14}$$

where I_{NN} is the isospin of the two-nucleon state. Finally, one takes combinations of isospin states to get pp and pn amplitudes

$$F^i(\mathrm{pp})=F^i(I_{\mathrm{NN}}=1) ,$$

$$F^i(\mathrm{pn})=\tfrac{1}{2}[F^i(I_{\mathrm{NN}}=1)+F^i(I_{\mathrm{NN}}=0)] . \tag{15}$$

These equations [(5), (8), (9), and (14)] form the basis of our fits in Sec. III. Again, the parameters are, for the real amplitudes, g_i and cutoffs Λ_i. In most cases, the masses will take on their experimental values (see Sec. III). We have chosen to use nonlinear cutoff parameters in Eq. (9d) rather than a sum over Yukawas of different ranges in order to minimize arbitrary cancellations that can result from a linear sum over couplings of different signs. It is easy to Fourier transform equation (9d) into r space

$$f^j_R(r)=\int\frac{d^3q}{(2\pi)^3}e^{iq\cdot r}f^j_R(q)$$

$$=\frac{g_j^2}{4\pi}\frac{\Lambda_j^2}{\Lambda_j^2-m_j^2}\left[\frac{\Lambda_j^2}{\Lambda_j^2-m_j^2}\left(\frac{e^{-m_jr}}{r}-\frac{e^{-\Lambda_jr}}{r}\right)-\frac{\Lambda_j}{2}e^{-\Lambda_jr}\right] . \tag{16}$$

For the imaginary amplitudes, the meson masses were chosen essentially arbitrarily, and the couplings $\bar{g}_i$ and the cutoffs $\bar{\Lambda}_i$ fit to data. In most cases, we were not able to determine both $\bar{m}_i$ and $\bar{\Lambda}_i$ independently.

III. DETAILS OF THE FITS TO THE NN DATA

One must fit to the pp and pn data simultaneously in addition to fitting all five invariants s, v, p, a, and t at once. (However, we fit real and imaginary parts separately.) Thus, the NN data at a given energy are represented by ten separate functions of q so as a minimum we will consider a fit with ten linear parameters and ten cutoffs.

For simplicity, we fit to NN amplitudes rather than directly to data but we examine the quality of the NN observables reproduced. The winter 1982 amplitudes of Arndt *et al.*[6] were used for the 200 MeV fits while the updated spring 1984 set was available for the 135 and 400 MeV fits. (The difference between the two sets is at most

TABLE I. Energy dependence of couplings.

		OBEP[a]	E lab (MeV)			
Meson	HM1	HEA	150	300	500	800
π	14.0	12.9	12.1	11.5	10.7	9.6
η	2.0	6.0	10.8	2.3	−3.2	−5.9
σ	6.3	4.7	6.3	5.1	4.1	3.0
ω	10.2	14.0	10.7	8.5	6.1	4.2

[a]One-boson-exchange potentials which fit the phase shifts after unitarization in the Schrödinger equation. [Holinde and Machleidt (HM1) (Ref. 15) and Holinde, Erklenz, and Alzetta (HEA) (Ref. 16)].

a few percent.)

The weights of different amplitudes were adjusted to obtain good fits to observables. For example, $s+v$ was fit along with s and v separately to insure a good fit to the cross section (since this involves some cancellation between s and v). In addition, it was necessary to increase the weight of the small a and t amplitudes. The fits were done at a range of q values corresponding to scattering angles of 0 to 90 deg in the center of mass.

To examine the energy dependence of the parameters, simple fits were done at lab energies of 150, 300, 500, and 800 MeV. The most important mesons in all of these fits were the pi, eta, sigma, and omega and their couplings are shown in Table I. (Note these fits involved ten mesons and were very similar to the 135 and 200 MeV fits in the following.) First, the pseudoscalar invariant is by far the largest and immediately determines the pi coupling constant. The resulting value is remarkably close to OBEP results (g^2 of about 12 for the fit vs 14) and has very little energy dependence. Likewise, the sigma and omega couplings agree well with OBEP's at low energies and then decrease very slowly with energy. The largest energy dependence is for the eta meson (isoscalar pseudoscalar), which is somewhat larger than OBEP at low energies, but it decreases and eventually changes sign with increasing energy. However, given the eta's much larger mass (550 vs 138 MeV) it's contribution is much smaller than the pion. This systematic energy dependence may be a sign of iteration effects beyond first Born approximation (in this pseudoscalar isoscalar channel).

The pion form factor Λ_π is ≈ 550 MeV. This somewhat low value may reflect the derivative coupling of the rho meson which is not included in our fits and serves to weaken the nonrelativistic tensor force from the pion. [Note the derivative coupling of the rho $\sigma^{\mu\alpha}q_\alpha(1)\cdot\sigma_{\mu\tau}q^\tau(2)$ should not be confused with a tensor Lorentz invariant $\sigma_{\mu\alpha}\cdot\sigma^{\mu\alpha}$.] The eta form factor varies with energy.

Detailed fits have been obtained at lab energies of 135, 200, and 400 MeV. Ten mesons proved adequate for the real parts of the amplitudes at 135 and 200 MeV. In addition, ten mesons were used in all of the fits to the imaginary amplitudes. The NN observables were not very sensitive to the quality of the fit to the imaginary amplitudes. At 400 MeV, additional mesons were needed to reproduce the complex behavior of the real tensor and axial vector amplitudes. The parameters are collected in Tables II, III, and IV, while the amplitudes are plotted in Figs. 1, 2, and 3.

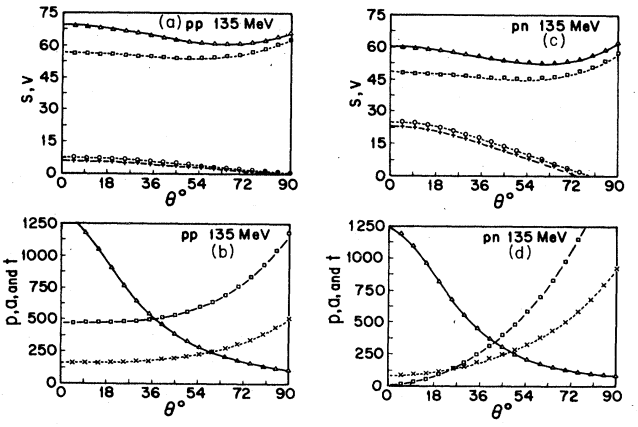

FIG. 1. Lorentz invariant form of the NN amplitudes in GeV^{-2} vs center of mass scattering angle at a lab energy of 135 MeV. Part (a) shows the s and v invariants [see Eqs. (2) and (3)] for pp scattering. The imaginary part of the v invariant calculated directly from the Arndt amplitudes (Ref. 6) is shown by the squares while the circles indicate the real part. Minus the scalar amplitude is shown by the triangles (imaginary) and crosses (real part). The lines are the fit using parameters from Table II. Part (b) shows the imaginary part of the p (triangles) and -50 times the small a (squares) and t (crosses) amplitudes. Parts (c) and (d) are as per (a) and (b), but for pn scattering.

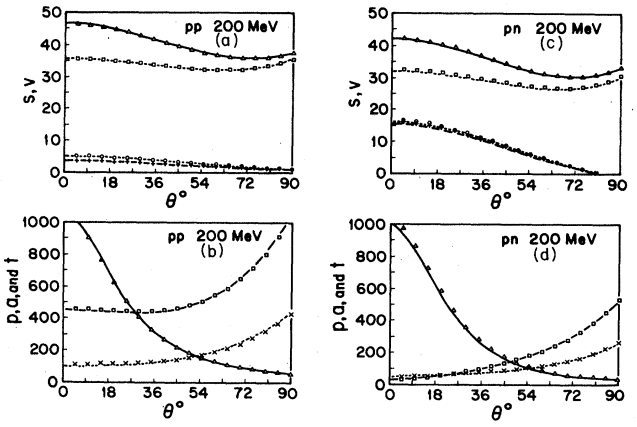

FIG. 2. NN amplitudes at $E_{\rm lab}=200$ MeV. See caption to Fig. 1. The smooth lines are the fit using Table III. The small a and t amplitudes have been multiplied by -100 in part (b) and -30 in part (d).

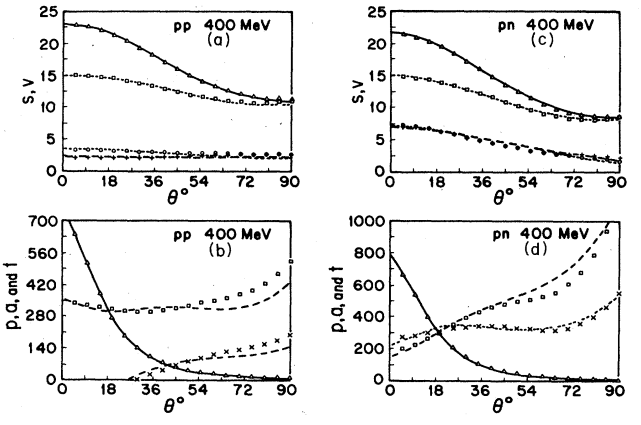

FIG. 3. NN amplitudes at $E_{\rm lab}=400$ MeV. See caption to Fig. 1. The smooth lines are calculated from Table IV, while the small a and t amplitudes have been multiplied by -300.

TABLE II. $E_{lab}=135$ MeV fit. A Fortran subroutine which uses these inputs or Tables III and IV and returns the relativistic invariants $F^s, \ldots, F^p$ is available from the author.

			Real				Imaginary		
Meson	Isospin	Coupling	m (MeV)	g^2	Λ (MeV)	$\overline{m}$ (MeV)	$\overline{g}^2$	$\overline{\Lambda}$ (MeV)
π	1	p	138	12.462	557.36	500	−6.335	1567.
η	0	p	550	9.742	2500.00	1000	3.679	652.
σ	0	s	500	−6.006	718.43	600	−4.012	558
ω	0	v	783	11.066	630.78	700	5.882	544
t_1	1	t	600	−0.319	432.67	750	0.525	2448
a_1	1	a	800	−2.088	444.57	1000	1.993	1662
δ	1	s	960	0.184	236.73	650	2.552	471
ρ	1	v	760	−0.343	547.59	600	−2.123	477
t_0	0	t	800	1.205	1322.82	750	−1.640	1382
a_0	0	a	1275	6.783	833.29	750	−3.567	1267

TABLE III. $E_{lab}=200$ MeV fit.

			Real				Imaginary		
Meson	Isospin	Coupling	m (MeV)	g^2	Λ (MeV)	$\overline{m}$ (MeV)	$\overline{g}^2$	$\overline{\Lambda}$ (MeV)
π	1	p	138	11.934	565.77	500	−3.732	994.92
η	0	p	550	7.395	1386.82	1000	4.567	1162.15
σ	0	s	500	−5.707	1018.96	600	−2.442	572.39
ω	0	v	783	9.875	835.09	700	3.837	584.66
t_1	1	t	600	−0.028	200.00	750	0.147	1139.03
a_1	1	a	800	−1.020	403.56	1000	0.440	865.60
δ	1	s	960	0.307	543.17	650	1.989	565.87
ρ	1	v	760	−0.529	917.19	600	−1.581	557.28
t_0	0	t	800	0.302	2500.00	750	−0.730	880.91
a_0	0	a	1275	2.052	1292.96	750	−1.709	933.15

TABLE IV. $E_{lab}=400$ MeV fit.

			Real				Imaginary		
Meson	Isospin	Coupling	m (MeV)	g^2	Λ (MeV)	$\overline{m}$ (MeV)	g^2	$\overline{\Lambda}$ (MeV)
π	1	p	138	11.334	526.02	500	−1.041	207.62
η	0	p	550	−4.662	212.14	1000	2.497	2412.39
σ	0	s	500	−4.520	1266.60	600	−1.360	2289.68
ω	0	v	783	7.032	1191.05	700	2.208	1172.29
t_1	1	t	600	2.947	200.00	750	−0.021	2500.00
a_1	1	a	800	−0.209	2500.00	1000	−0.105	1042.87
δ	1	s	960	−0.454	2500.00	650	1.069	1211.56
ρ	1	v	760	−0.391	250.71	600	−0.772	1327.56
t_0	0	t	800	−0.351	2500.00	750	−0.206	838.87
a_0	0	a	1275	7.300	331.23	750	−0.444	2330.57
t_1'	1	t	200	−0.316	254.74			
t_0'	0	t	200	0.015	313.65			
a_1'	1	a	250	−0.022	200.00			
a_0'	0	a	250	−0.304	2500.00			
σ'	0	s	1000	0.513	216.16			
δ'	1	s	400	0.073	245.52			

The s and v amplitudes are the most important for elastic scattering. At 400 MeV (see Fig. 3), the real part of s is seen to fall more rapidly with q than the v amplitude. However, as the energy is lowered (Figs. 1 and 2), both s and v start to rise at back angles (this is fit with exchange contributions). The absorptive parts of both s and v are seen to be primarily isoscalar.

The p amplitude is one to two orders of magnitude larger than any of the others and almost entirely real (the small imaginary part is not shown). The small pion mass is clearly evident in the rapid q dependence of p. Also shown in Figs. 1—3 are the very small a and t amplitudes (multiplied by a large factor). At 135 and 200 MeV, a and t are seen to rise smoothly with q. However, at 400 MeV, the q dependence of these amplitudes is more complex. This necessitated adding more terms in the fit and resulted in the largest fitting errors of any of the amplitudes (see Fig. 3). Such errors may be significant in some inelastic transitions which are sensitive to a and t. However, a and t are very small indeed at this energy and one should also be worried how well the a and t amplitudes (we are fitting) are determined by the NN data.

To judge the quality of our fits to the amplitudes the resulting NN observables have been calculated and compared to the observables predicted by the Arndt amplitudes directly. Results are shown in Figs. 4—6 for the cross section, polarization, depolarization, A_{yy}, A, and R, as defined in Ref. 13. The fit does a good job of reproducing the NN observables.

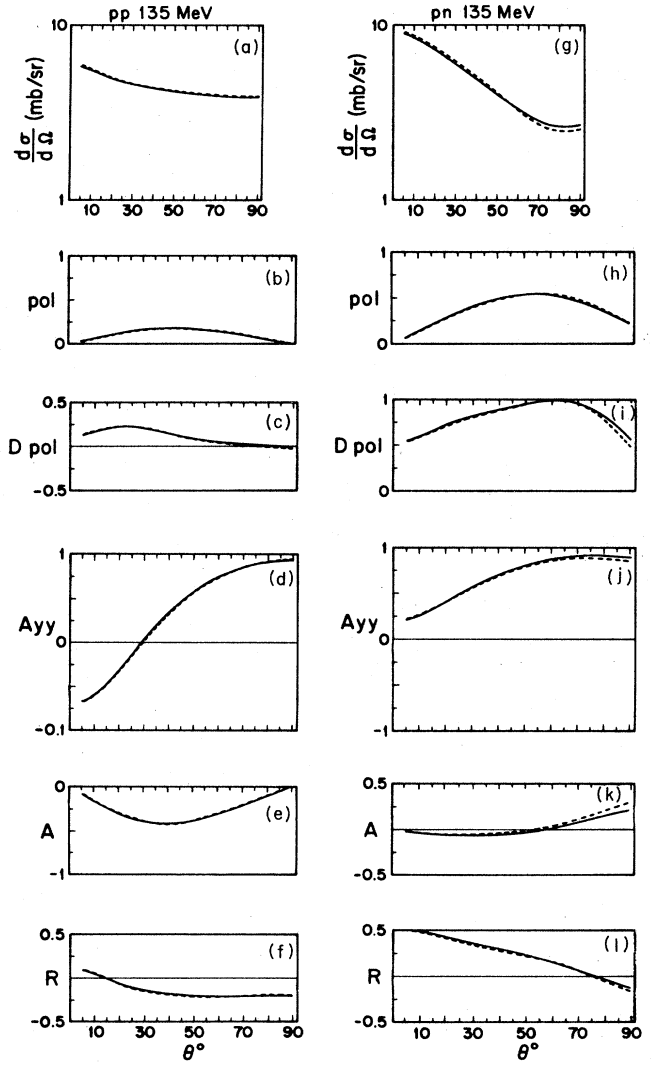

FIG. 4. NN scattering observables at $E_{\text{lab}}=135$ MeV vs center of mass scattering angle. The dashed lines show the observables calculated from the Arndt amplitudes (Ref. 6) directly while the solid lines are calculated from the fits. Part (a) shows the log of the differential cross section for pp scattering. Spin observables (using the notation of Ref. 13) are shown in parts (b) (polarization), (c) (depolarization), (d) (A_{yy}), and the triple scattering parameters (e) (A), and (f) (R). Finally, parts (g)—(l) are as per (a)—(f) but for pn scattering.

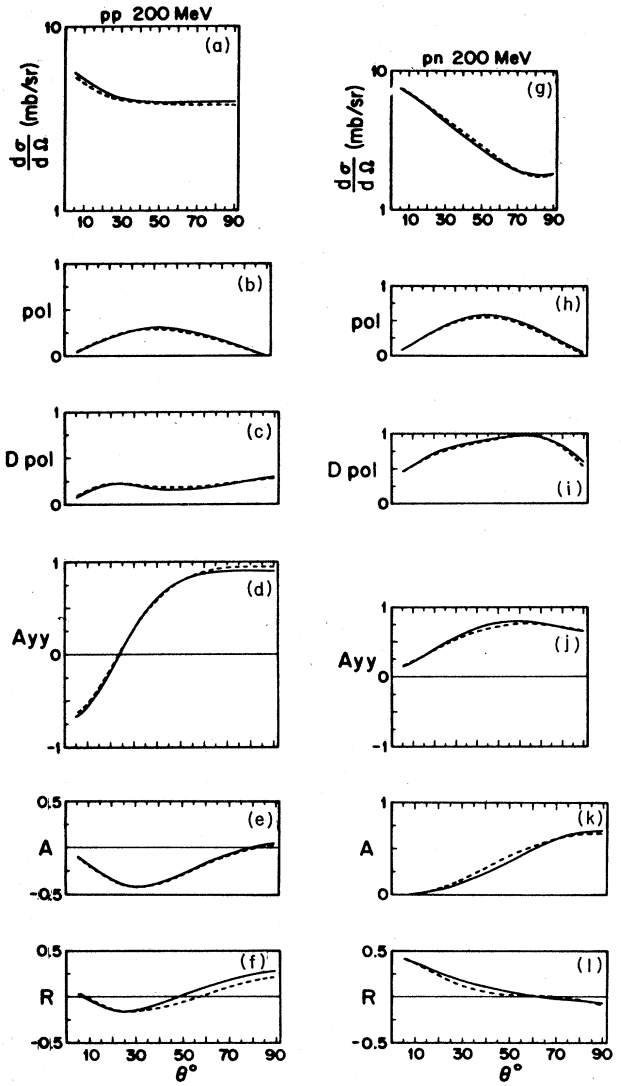

FIG. 5. NN observables at $E_{\text{lab}}=200$ MeV. See caption to Fig. 4.

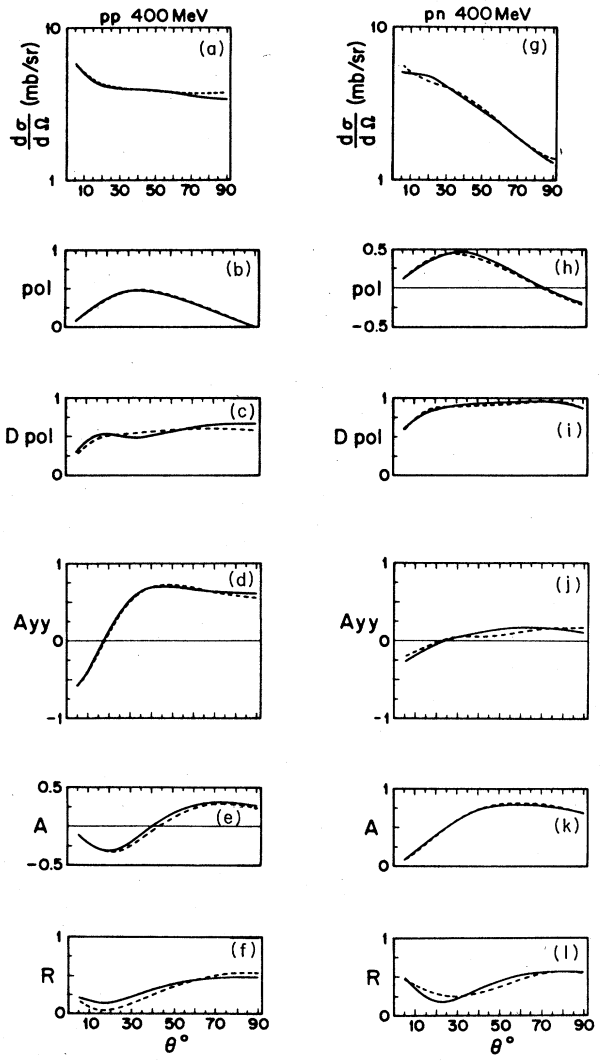

FIG. 6. NN observables at $E_{lab}=400$ MeV. See caption to Fig. 4.

IV. DIRECT VERSUS EXCHANGE CONTRIBUTIONS

The model provides a separating into direct and exchange contributions. Since the couplings are close to OBEP values, this breakdown is expected to be similar for a full OBEP.

(a) The pseudoscalar invariant is almost completely direct. Because the pion is so light, its exchange contribution to p is damped. Other mesons make only a small contribution to p because of their larger masses and smaller couplings.

(b) The s and v invariants at 200 MeV are about 75% direct. As the energy increases, both s and v become dominated by the direct terms only.

Note the direct and exchange contributions have the *same* sign. This lack of cancellation is due to the interplay of sigma and omega exchange contributions. While the exchange contribution of the sigma to s is indeed of opposite sign (to the direct term), the total exchange contribution is dominated by the omega because C_{vs} is four times lager than C_{ss}. These signs for the total exchange contributions are a common feature of most relativistic Hartree-Fock calculations[14] and may significantly reduce the sensitivity to how the exchange terms are treated.

(c) The small amplitudes a and t involve important exchange contributions. In the model, this is the only way to reproduce the increase of these amplitudes with q.

TABLE V. Direct and exchange separation of forward amplitudes.

	Direct only[a]	Direct and Exchange[b]
	$E_{lab}=100$ MeV	
s	-61 (GeV^{-2})	-92 (GeV^{-2})
v	43	78
p	1509	1503
a	4	-15
t	3	-5
	$E_{lab}=400$ MeV	
s	-21	-23
v	13	15
p	620	623
a	-1	-1
t	0	0.1

[a]The real part of Eq. (8) is listed multiplied by $(E_{c.m.}/2P_{c.m.})$ for $q=\theta_{c.m.}=0$.
[b]The imaginary part of Eq. (5) is listed (because of the explicit factor of (i) also at $\theta_{c.m.}=0$.

Table V shows the total and direct only contributions to the forward ($\theta_{c.m.}=0$) pp amplitudes.

V. IMPULSE APPROXIMATION OPTICAL POTENTIAL

The relativistic impulse approximation (RIA) has proven to be remarkably useful in describing N-nucleus scattering at 500 MeV and above. This approximation starts with a covariant representation of the NN amplitudes such as Eqs. (2) and (3) and then strips the spinors away and takes the appropriate traces over the densities of the target to get Eq. (4). This is a generalization of the nonrelativistic "$\tau\rho$" approach and depends explicitly on the operator form of the NN amplitudes, Eq. (3), not just on these spinor matrix elements in Eq. (2). Clearly, the NN data only give you information about Eq. (2), while Eq. (3) is a prescription for a model dependent Dirac operator. In general, there are an infinite number of different operators with the same spinor matrix elements. We emphasize the RIA optical potential in Eq. (4) (and observables calculated with it) depends explicitly on the form chosen in Eq. (3).[3]

Since the RIA optical potential is arbitrary, what accounts for its success at high energies? Clearly, there is important physics buried in the postulated form of the NN amplitudes [Eq. (3)]. This form is completely local (no factors of a momentum dotted into a gamma matrix appear explicitly). The agreement with data at high energies suggest this is a good approximation. But, as the energy is decreased, the NN amplitudes cannot be completely local. At a minimum, there must be exchange nonlocalities. Indeed, the RIA optical potential of Eq. (4) diverges at energies below 100 MeV and becomes much

greater than phenomenological potentials. We believe this is because Eq. (3) is an inappropriate representation of the amplitudes at low energies.

With our simple model of the NN amplitudes, we are in a position to examine different forms in place of Eq. (3). The most important ambiguity is the difference between pseudoscalar and pseudovector π-N coupling. Consider replacing the p invariant in Eq. (3) with

$$\lambda^{pv}=\gamma^5 q/2M \ . \tag{17}$$

Use of the Dirac equation for the spinors in Eq. (2) shows that Eq. (17) with the same F^p (which we could rename $F^{pv}=F^p$) will give identical spinor matrix elements [Eq. (2)] of the NN amplitudes. Therefore, our fit of the data is just as valid with γ^5 replaced by Eq. (17), and no two-nucleon experiment can distinguish between them.

However, let us now calculate an optical potential to first order in the NN t matrix which uses Eq. (17). For elastic scattering from a spin zero target there are only scalar, vector, and (a very small) tensor potentials. Therefore, this change in the p invariant only effects its exchange contribution to these potentials. The direct terms are unchanged. One calculates a 4×4 Dirac matrix for the exchange optical potential, $U_{\rm ex}$. In infinite nuclear matter, this is

$$U_{\rm ex}(q=0)=2\pi\left[\frac{E_{\rm c.m.}p}{p_{\rm c.m.}M}\right]\sum_{2}^{\rm occupied} f^p(Q)(-)^{I_{\rm NN}}(\tau_1\cdot\tau_2)\lambda^{pv}(Q)\,|\,U_2\rangle\langle U_2\,|\,\lambda^{pv}(Q) \ . \tag{18}$$

Here, the sum over spins of the target wave functions can be replaced with a projection operators, $(\not p_2+M)/2M$. The scalar and vector components of $U_{\rm ex}$ can be projected by taking appropriate traces. We also chose to make an impulse approximation and assume the target nucleons are at rest. This gives a scalar U_s and a vector U_0 contribution

$$\begin{aligned} U_s&=-4\pi\left[\frac{pE_{\rm c.m.}}{2Mp_{\rm c.m.}}\right]\left[\frac{Q_\mu^2}{4M^2}\right]\frac{3f^p(Q)}{2}\rho_s \ , \\ U_0&=-4\pi\left[\frac{pE_{\rm c.m.}}{2Mp_{\rm c.m.}}\right]\left[\frac{Q_\mu^2-2Q_0^2}{4M^2}\right]\frac{3f^p(Q)}{2}\rho_b \ . \end{aligned} \tag{19}$$

If the γ^5 invariant is used instead, one would have

$$\begin{aligned} U_s&=-4\pi\left[\frac{pE_{\rm c.m.}}{2Mp_{\rm c.m.}}\right]\frac{3f^p(Q)}{2}\rho_s \ , \\ U_0&=4\pi\left[\frac{pE_{\rm c.m.}}{2Mp_{\rm c.m.}}\right]\frac{3f^p(Q)}{2}\rho_b \ . \end{aligned} \tag{20}$$

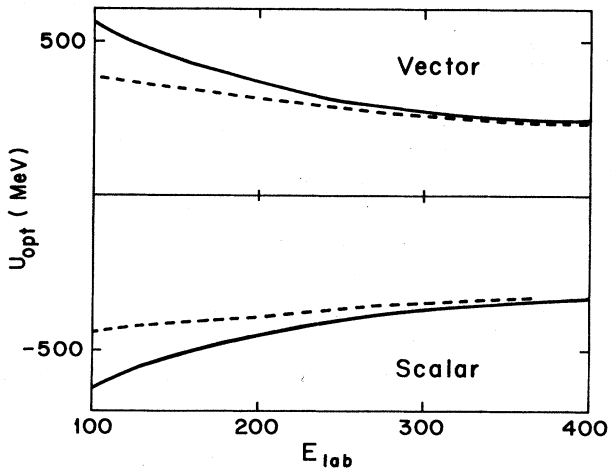

FIG. 7. Optical potentials in infinite nuclear matter. ($\rho_B=0.16$ fm^{-3}, $\rho_s=0.15$ fm^{-3}) vs projectile energy. The solid lines use a pseudoscalar p invariant, Eq. (20), while the dashed curves use a pseudovector invariant, Eq. (19).

Equation (20) is equivalent to the Fierz expression, Eq. (14), multiplied by the density. However, for λ^{pv}, the momentum dependence of the invariant used in Eqs. (17) and (19) invalidates a simple Fierz matrix relation.

Comparing Eq. (19) to (20), we see that the pseudovector invariant reduced the exchange contribution of p by a factor

$$\approx\pm\frac{Q^2}{4M^2} \ , \tag{21}$$

which is much less than one. The optical potentials from Eqs. (19) and (20) are shown in Fig. 7. At high energies they agree. But as the energy decreases, the pseudoscalar equation (20) diverges due to the very large pion exchange contribution. This expression agrees with the simple RIA results and disagrees with phenomenological fits to elastic scattering data.[5]

In contrast, the pseudovector results have a very small exchange contribution from the pion. Therefore, they are almost constant with energy, in good agreement with phenomenological fits. We conclude that the unrealistic behavior of the original RIA optical potential (at low energies) is due to the completely local expression for the NN amplitudes, Eq. (3).

This can be cured simply by including the exchange nonlocalities implied by a pion with pseudovector coupling. We emphasize, this is not a medium modification. In fact, Pauli blocking was seen to have almost no effect on the large real potentials although it substantially improves the imaginary potential.[9]

VI. CONCLUSIONS

In this paper we have developed a simple model of the NN interaction for use in N-nucleus scattering calculations. The interchange of a number of mesons was considered (in first Born approximation). The (complex) couplings and form factors have been adjusted to reproduce a relativistic form of the NN amplitudes without iteration.

The model provides an analytic representation of the amplitudes which may be useful in relativistic inelastic calulations. Detailed fits were presented at 135, 200, and 400 MeV. These analytic fits may allow a detailed exam-

ination of sensitivities to different off-shell extrapolations. The model separation of direct and exchange contributions involves no sensitive cancellations (in contrast to nonrelativistic results) and allows one to systematically improve the treatment of exchange in N-nucleus scattering.

Furthermore, there are a number of important advantages of the current work over the conventional approach of Love and Franey. There is a simple relationship between the individual Lorentz invariant amplitudes and the mesons exchanged. The parameters may be meaningful since they are close to OBEP results and have a systematic and small energy dependence. Finally, the interaction is Lorentz covariant and allows one to treat strong relativistic optical potentials.

A new feature of relativistic approaches is their dependence on the form of the operator used to represent the NN interaction. We have calculated optical potentials using both pseudoscalar and pseudovector couplings for the p invariant. The pseudovector calculations have much less energy dependence. So we conclude the divergences of earlier RIA calculations (at low energy) stem from an inappropriate representation of the NN amplitudes.

ACKNOWLEDGMENTS

The warm hospitality of the Colorado University Cyclotron Laboratory is gratefully acknowledged as are useful conversations with J. Shepard, E. Rost (who also provided assistance with search codes), and J. McDermott (who provided calculations of the NN observables). This work was supported in part by the U.S. Department of Energy.

*Permanent address: Center for Theoretical Physics and Department of Physics, Massachusetts Institute of Technology, Cambridge, MA 02139.

[1]J. A. McNeil, J. Shepard, and S. J. Wallace, Phys. Rev. Lett. **50**, 1439 (1983); **50**, 1443 (1983).

[2]C. J. Horowitz and Brian D. Serot, Nucl. Phys. **A368**, 503 (1981); J. D. Walecka, Ann. Phys. (N.Y.) **83**, 491 (1974).

[3]P. L. Adams and M. Bleszynski, Phys. Lett. **136B**, 10 (1984).

[4]J. A. McNeil, L. Ray, and S. J. Wallace, Phys. Rev. C **27**, 2123 (1983).

[5]L. G. Arnold, B. C. Clark, and R. L. Mercer, Phys. Rev. C **19**, 917 (1979); L. G. Arnold, B. C. Clark, R. L. Mercer, and P. Schwandt, *ibid.* **23**, 1949 (1981).

[6]R. A. Arndt and D. Roper, VPI and SU Scattering Analysis Interactive Dialin Program and Data Base.

[7]C. J. Horowitz and Brian D. Serot, Phys. Lett. **137B**, 287 (1984).

[8]W. G. Love and M. A. Franey, Phys. Rev. C **24**, 1073 (1981).

[9]C. J. Horowitz, Massachusetts Institute of Technology Report CTP 1144, 1984.

[10]S. Wallace, private communication.

[11]J. D. Bjorken and S. D. Drell, *Relativistic Quantum Mechanics* (McGraw-Hill, New York, 1964).

[12]M. Fierz, Z. Phys. **104**, 533 (1937).

[13]W. O. Lock and D. F. Measdy, *Intermediate Energy Nuclear Physics* (Methuen, London, 1970), p. 164.

[14]C. J. Horowitz and Brian D. Serot, Nucl. Phys. **A399**, 529 (1983); M. Jaminon, C. Mahaux, and P. Rochus, Phys. Rev. C **22**, 2027 (1980).

[15]K. Holinde and R. Machleidt, Nucl. Phys. **A247**, 495 (1975).

[16]K. Holinde, K. Erkelenz, and R. Alzetta, Nucl. Phys. **A194**, 161 (1972).